Continuous evolution of the inplane magnetic anisotropies with thickness in epitaxial Fe films

M. Gester, C. Daboo, R. J. Hicken, S. J. Gray, A. Ercole et al.

Related Articles

Magnetic properties of copper hexadecaphthalocyanine (F16CuPc) thin films and powders
J. Appl. Phys. 113, 013914 (2013)

Low temperature oxidation mechanisms of nanocrystalline magnetite thin film
J. Appl. Phys. 113, 013510 (2013)

In situ control of electronic phase separation in La1/8 Pr4/8Ca3/8MnO3/PNM-PT thin films using ferroelectric-poling-induced strain
J. Appl. Phys. 113, 013705 (2013)

Spin precession modulation in a magnetic bilayer
Appl. Phys. Lett. 101, 262406 (2012)

Alternating domains with uniaxial and biaxial magnetic anisotropy in epitaxial Fe films on BaTiO3
Appl. Phys. Lett. 101, 262405 (2012)

Additional information on J. Appl. Phys.

Journal Homepage: http://jap.aip.org/

Journal Information: http://jap.aip.org/about/about_the_journal

Top downloads: http://jap.aip.org/features/most_downloaded

Information for Authors: http://jap.aip.org/authors

Continuous evolution of the in-plane magnetic anisotropies with thickness in epitaxial Fe films

M. Gester,[a] C. Daboo, R. J. Hicken,[b] S. J. Gray, A. Ercole, and J. A. C Bland

Cavendish Laboratory, University of Cambridge, Madingley Road, Cambridge CB3 OHE, United Kingdom

We have studied the evolution of the magnetic in-plane anisotropy in epitaxial Fe/GaAs films of both (001) and ($\bar{1}$10) orientation as a function of the Fe layer thickness using the longitudinal magneto-optic Kerr effect and Brillouin light scattering. Magnetization curves which are recorded *in situ* during film growth reveal a continuous change of the net anisotropy axes with increasing film thickness. This behavior can be understood to arise from the combination of a uniaxial and a cubic in-plane magnetic anisotropy which are both thickness dependent. Structural analysis of the substrate and Fe film surfaces provides insight into the contribution of atomic steps at the interfaces to the magnetic anisotropy. Changing the degree of crystalline order at the Fe–GaAs interface allows us to conclude that the magnetic anisotropies are determined by atomic scale order. © *1996 American Institute of Physics.* [S0021-8979(96)04613-0]

I. INTRODUCTION

In thin film systems, magnetic anisotropies profoundly influence the magnetic behavior.[1] Therefore, studies of the magnetic anisotropies in single ferromagnetic films are a key step in fully understanding the behavior of coupled multilayer systems which are composed of such single layers. This involves careful characterization of the film structure and the interface morphology which strongly affect the magnetic anisotropies. There are many different mechanisms which contribute to the magnetic anisotropy energy. The magnetocrystalline anisotropy reflects the crystalline structure of an epitaxial film. Due to the spin–orbit interaction, the energy of a spin depends on its orientation with respect to the crystal axes. Additional contributions to the magnetocrystalline anisotropy energy arise from the reduced coordination number of surface or step atoms.[2] Strain in epitaxial films can give rise to magnetoelastic anisotropy due to the distortion of the crystal lattice.[3] Shape anisotropy arises from the dipolar fields which, in the case of a homogeneously magnetized film, force the magnetization to lie in the plane. This effect is reduced by interface roughness.[4]

It is a challenging task to experimentally separate the contributions from the above mechanisms from the total magnetic anisotropy in thin films. In some cases only one mechanism has been considered while neglecting other terms.[5,6] More generally, separation is possible when the thickness dependence or the symmetry is different for individual anisotropy contributions. This has been done successfully in the case of surface and step anisotropies for Fe/W(110) films[7] and for strain and surface anisotropies in fcc Co films on Cu(110).[8] For the latter system, it has recently been shown that in-plane, perpendicular, and bulk anisotropy energies may not be simply additive as is usually assumed.[9]

We carried out the first *in situ* study of the magnetic anisotropies in the Fe/GaAs system which is of considerable interest for applications.[10] All previous studies of magnetic properties in Fe/GaAs films were carried out *ex situ* on a number of different samples of fixed thickness. Magnetic anisotropies of oxidized or Al-coated Fe films deposited on either GaAs(001) or ($\bar{1}$10) were investigated by Prinz and co-workers using *ex situ* techniques such as ferromagnetic resonance (FMR) and vibrating sample magnetometry (VSM).[11,12] The magnetization reversal process in Fe/GaAs(001) films was studied using the magneto-optic Kerr effect (MOKE).[13,14] No evidence for dominating perpendicular anisotropy was found when studying the extraordinary Hall effect in Fe/GaAs films.[15] This is in contrast to several monolayer thick Fe films on Ag(001), for which a strong perpendicular anisotropy was predicted[16] and observed.[17]

In this article, we report a continuous evolution of the in-plane magnetic anisotropies (IPMA) and the magnetization in epitaxial Fe films on GaAs substrates of both (001) and ($\bar{1}$10) orientation. We use the longitudinal MOKE in order to monitor magnetization curves along different crystallographic directions *in situ* during deposition. These measurements yield a qualitative thickness dependence of the IPMA for one single film on the same surface avoiding any uncertainties due to different substrate morphologies. The crystallographic structure of the Fe film surfaces is characterized using electron diffraction [low-energy electron diffraction (LEED) and reflection high-energy electron diffraction (RHEED)] as described in detail elsewhere.[18] After the samples are protected with a Cr overlayer and removed from the growth system, the IPMA fields are quantitatively determined using Brillouin light scattering (BLS). In both, (001) and ($\bar{1}$10) oriented Fe films, we observe a cubic and a uniaxial IPMA. With increasing film thickness the strength of these two contributions to the total IPMA varies differently. This leads to a directional change of the easy and hard magnetization axes with respect to the crystallographic axes in the film plane as the Fe layer grows thicker.

This article is organized as follows: The treatment of the GaAs substrate surfaces prior to Fe deposition in vacuum

---

[a] Present address: Department of Physics, University of York, York YO1 5DD UK; Electronic mail: mg21@unix.york.ac.uk
[b] Present address: Department of Physics, University of Exeter, Exeter EX4 4QL, UK.

and the procedure of the Fe growth are described in Sec. II. Results on the evolution of the magnetization curves and the IPMA as a function of Fe film thickness obtained with *in* and *ex situ* magnetometry techniques are presented in Sec. III. In Sec. IV, the *in situ* MOKE loops are analyzed in terms of the anisotropy energy density and the thickness dependence of the magnetic properties and possible origins of the uniaxial IPMA are discussed.

II. EXPERIMENT

The majority of the Fe films studied here were deposited onto commercial GaAs wafers. In a few cases, As-capped epilayers and special etch stop buffer layers grown on the commercial wafers were used as substrates to produce samples for further investigations using transmission electron microscopy based techniques.[14,19] It has been reported previously that heating of the GaAs substrates to temperatures above 600 °C prior to material deposition desorbs the native surface oxide and yields an ordered surface structure.[20] However, we were unable to observe LEED spots after this treatment and Auger spectroscopy revealed that the surface oxide was desorbed but a considerable amount of carbon remained on the surface. Only after bombardment with 500 eV Ar^+ ions and subsequent annealing of the substrate above 600 °C for at least half an hour the surfaces were found to be free of any contaminations and diffraction spots were visible.[18] In the case of GaAs(001), we observed LEED patterns for a reconstructed surface similar to previously published images.[21] These LEED images and the rectangular diffraction pattern observed in the case of GaAs($\bar{1}$10) made it possible to absolutely determine the crystallographic directions. Fe films were deposited onto GaAs substrates treated by either method in order to study the influence of the substrate surface structure on the properties of the magnetic films.

Fe was evaporated at a rate of approximately 1 Å/min and at a pressure below 5×10^{-10} mbar from the tip of a high purity wire which was heated by electron bombardment. The Fe evaporator was normal to the substrate surface to eliminate possible uniaxial magnetic anisotropies induced by oblique incidence evaporation as reported for Fe/MgO(001).[22] During growth all substrates were held at 150 °C, which is the average of temperatures reported previously to yield good epitaxial films.[20,23] The thickness was monitored by a quartz crystal balance which was calibrated using a profilometer on completed thick films. We estimate that thicknesses determined by this method are accurate to within 10%.

For Fe films deposited onto sputter-annealed GaAs(001) substrates, a LEED pattern of cubic symmetry was present for all thicknesses. Sharp LEED spots were observed for incident electron energies corresponding to the Bragg condition for the three-dimensional reciprocal Fe lattice. However, for other energies the spots were broadened along the ⟨110⟩ directions giving rise to cross-shaped diffraction features which indicate an irregular distribution of steps with edges parallel to all four ⟨110⟩ directions on the surface. With increasing Fe film thickness, these cross-shaped diffraction features become sharper and gradually split into four spots due to an increasing number of steps, which eventually leads
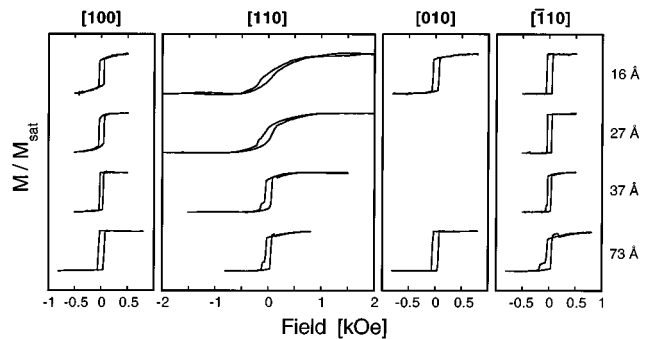

FIG. 1. *In situ* MOKE loops along four principal crystallographic directions for an Fe/GaAs(001) film up to 73 Å thick.

to the formation of extended slope regions.[18] In the case of Fe/GaAs($\bar{1}$10) films, LEED spots were found to have elliptical shape indicating that the number of steps with edges parallel to the [001] direction is higher than for the [110] direction. With increasing film thickness, the diffraction spots become sharper, i.e., the step density decreases and the film surface becomes flatter as previously observed.[24]

For both GaAs orientations, Fe films deposited onto heated-only substrates did not show a diffraction image until the thickness exceeded approximately 15 Å, indicating more disordered growth. For thicker Fe films the LEED spots showed the same features as in the case of films grown on sputter-annealed substrates.

In situ MOKE measurements were made on the samples during growth using an electromagnet with a maximum field of 2.1 kOe, and an intensity stabilized HeNe (633 nm) laser in the longitudinal MOKE geometry. Deposition was halted during each sequence of MOKE measurements and a series of loops were taken at different in-plane orientations of the sample with respect to the applied field, corresponding to the expected principal anisotropy axes. After removal of the samples from the chamber *ex situ* MOKE measurements were used to verify the final anisotropy state observed *in situ*. *Ex situ* Brillouin light scattering (BLS) measurements were used to quantify the magnetic properties of the films.[25]

III. RESULTS

A. (001) surface

A set of typical *in situ* $M-H$ curves for an Fe film of 73 Å total thickness deposited onto sputter-annealed GaAs(001) is shown in Fig. 1. For each loop the MOKE intensity is normalized to the signal obtained in the saturated state. No magnetic signal can be detected for films thinner than 10 Å. Above this thickness, an almost linear field dependence of the magnetization is observed independently of the direction of the applied field (not shown in the figure). The magnetization cannot be saturated with fields up to the maximum available field of 2.1 kOe suggesting a paramagnetic state. At an Fe thickness of about 15 Å, a uniaxial IPMA has developed with the hard and easy axes parallel to [110] and [$\bar{1}$10], respectively, which dominates the anisotropy behavior. After a gradual transition in the thickness range of 30–50 Å two easy axes are present (at 73 Å in Fig. 1). They are almost 90°
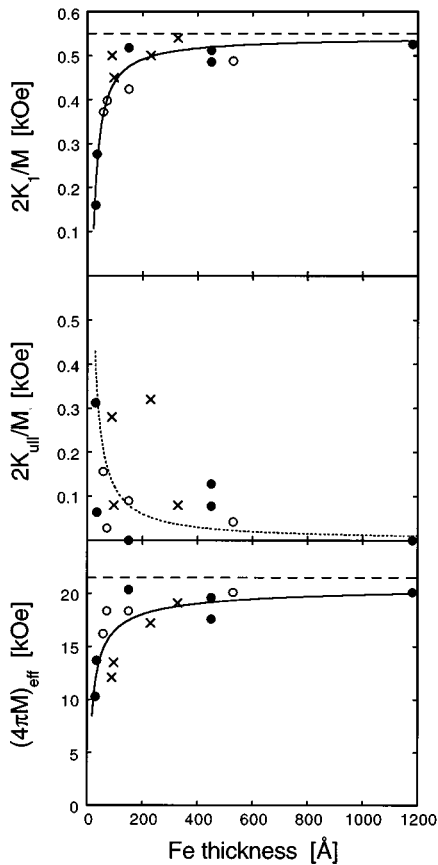
FIG. 2. The anisotropy fields and the effective demagnetizing field for nine Fe/GaAs(001) samples derived from spin wave data obtained with BLS. The solid and open circles denote sputter-annealed and heated-only GaAs substrates, respectively. The crosses are taken from Ref. 20 and the dashed lines represent the values for bulk Fe. The solid lines serve as guide to the eye and the dotted line is proportional to t^{-1}.

apart and parallel to $\langle 100 \rangle$ as in bulk Fe indicating a state of dominating cubic IPMA. This behavior is observed for all samples, however, the absolute thickness range in which this change occurs depends on the substrate and growth conditions.

The steplike features visible in the MOKE loops for fields applied close to the $\langle 110 \rangle$ axes arise from the transverse magnetization component which can partly be sensed for the analyzer angle used, approximately 1° away from extinction with respect to the polarization direction of the incident light.[26] These steps are caused when the magnetization in the film plane jumps over each of the two hard axes indicating the presence of cubic IPMA.[14]

Within the coherent rotation model, absolute values of the cubic and the uniaxial anisotropy fields could in principal be determined from the saturation fields for the hard axis directions. However, from the MOKE loops shown in Fig. 1, one can see that this method will not be very accurate and instead the IPMA fields are determined *ex situ* using BLS for Fe films in the thickness range of 20–1200 Å[25] which were protected against oxidation with a Cr layer.

The IPMA and the demagnetizing fields obtained from fitting the BLS data to calculated spin wave frequencies are plotted as a function of thickness in Fig. 2.[25] $(4\pi M)_{\text{eff}}$ is the
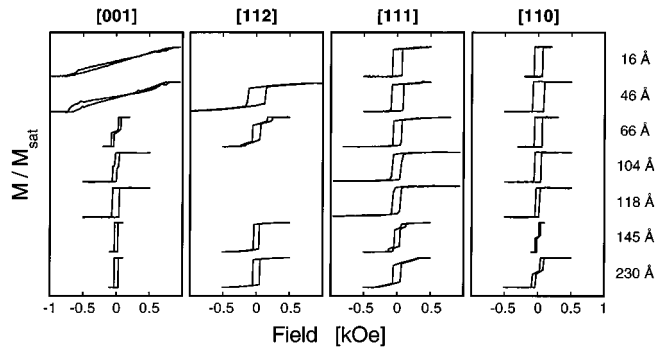

FIG. 3. *In situ* MOKE loops along four principal crystallographic directions for an Fe/GaAs($\bar{1}$10) film up to 230 Å thick.

effective demagnetizing field which contains any perpendicular surface anisotropy contributions that may exist, and K_1 and $K_{u\parallel}$ are the cubic and in-plane uniaxial anisotropies. The solid and open circles denote Fe films deposited onto sputter-annealed and heated-only GaAs(001) substrates, respectively. For comparison, the crosses mark FMR results obtained by Krebs *et al.*[20] As the film thickness increases, the cubic IPMA and the magnetization clearly approach the values for bulk Fe (dashed lines) while the uniaxial IPMA contribution drops to zero. Also, the three parameters appear to vary over roughly the same length scale. It is particularly important to note that there is much more scatter in the data for the uniaxial anisotropy, emphasizing how sensitive $K_{u\parallel}$ is to the specific substrate and growth conditions which give rise to varying degrees of macroscopic and microscopic roughness.

B. ($\bar{1}$10) surface

A typical set of normalized *in situ* $M-H$ curves for an Fe film of 230 Å final thickness deposited onto ion-bombarded and annealed GaAs($\bar{1}$10) is presented in Fig. 3. A clear magneto-optic signal can be detected from ~10 Å onwards, which shows an easy axis loop for the [110] direction and a hard axis loop for the [001] direction, in contrast to bulk Fe. As the film grows thicker, the saturation field for the loop along the [001] direction decreases, and steps develop which are typical of an intermediate magnetization axis. Also, the coercive field strength of the easy axis loop in the [110] direction decreases slightly as expected from a coherent rotation model in the presence of two competing anisotropies as shown in the next section. With increasing thickness a square shaped MOKE loop also appears for the [001] direction at an Fe thickness of about 120 Å, indicating the simultaneous presence of two easy axes. This behavior suggests that at least two competing anisotropy energies are present in the film which favor alignment of the magnetization along different crystal axes each of which could have a significant thickness dependence. Beyond 120 Å, the roles of the [110] and [001] directions are interchanged. Now the loop for [001] stays square and the stepped $M-H$ loop is observed along [110]. The magnetization curves for the two intermediate crystallographic directions ([112], $\varphi = 35.26°$ and [111], $\varphi = 54.74°$) undergo changes of their shape, too.
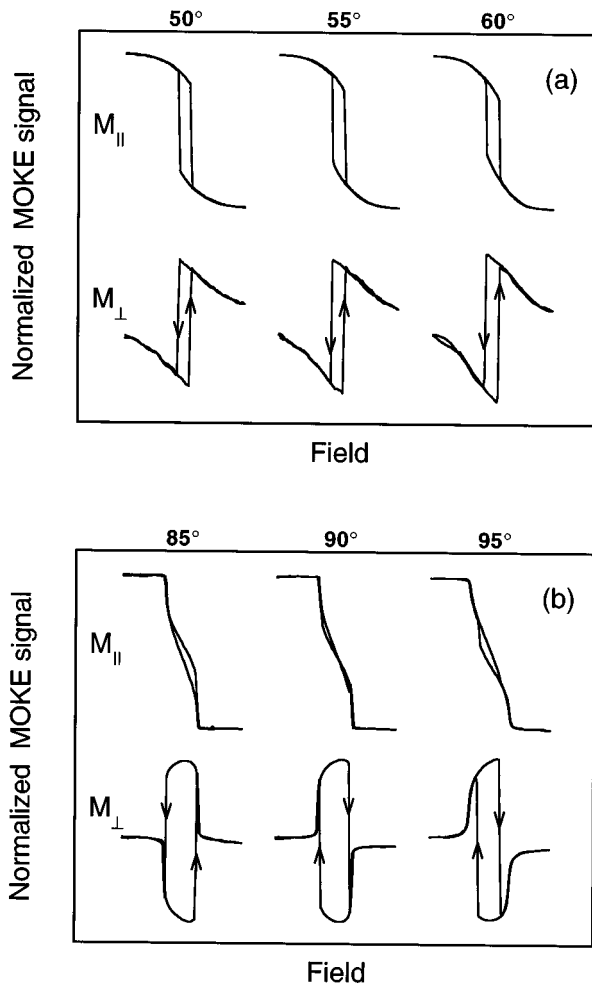
FIG. 4. The magnetization component parallel $M_\parallel$ and perpendicular $M_\perp$ to the applied field in the plane of a 230-Å-thick Fe/GaAs($\bar{1}$10) film measured with *ex situ* MOKE. The arrows mark the sense of the magnetization rotation which changes at the hard axis near 90° corresponding to the [110] direction.

FIG. 5. The anisotropy fields and the effective demagnetizing field for Fe/GaAs($\bar{1}$10) samples: ●—this study, ×—from Ref. 28, ▲—Al-coated and △ oxidized samples from Ref. 12. The dashed lines represent the values for bulk Fe and the solid lines serve as guide to the eye.

The presented sequence of loops implies that the hard axis orientation changes continuously from the [001] direction toward the [111] direction and possibly on to the [110] direction, while the easy axis suddenly switches from the [110] to the [001] direction at some critical thickness.

The direction of the hard anisotropy axis in completed films was determined using *ex situ* MOKE. During reversal of an applied field, the sense of rotation of the magnetization changes when the direction of the applied field corresponds to a hard or easy axis. This can be determined from MOKE loops which measure the component of magnetization perpendicular to the applied field direction ($M_\perp$).[14] In Fig. 4, we present two sequences of *ex situ* MOKE loops for both components of the magnetization in the film plane, $M_\parallel$ and $M_\perp$, for an Fe film of 150 Å thickness. Figure 4(a) shows loops at 5° intervals around 55°—the [111] direction, while Fig. 4(b) shows loops at 5° intervals around 90°—the [110] direction. The arrows on the $M_\perp$–H loops indicate the rotation sense of the perpendicular magnetization component. A change in rotation sense occurs only close to 90°, implying that the
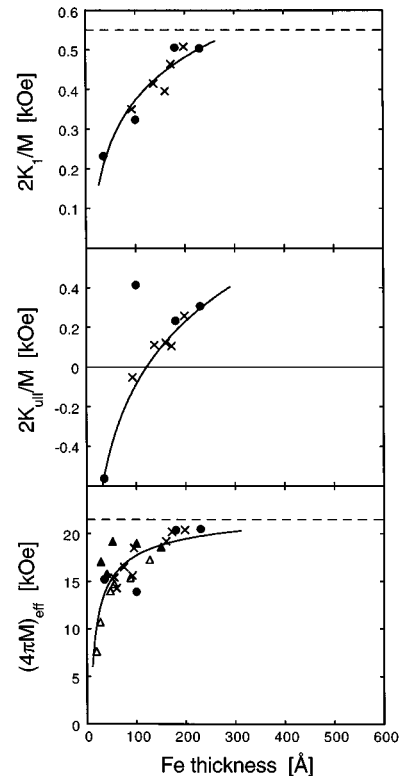
hard axis lies along the [110] direction and not along the [111] direction as in bulk Fe.

The cubic and uniaxial anisotropy fields and the effective demagnetizing field derived from BLS measurements are shown in Fig. 5 together with the results from other authors. Again the magnetization and cubic anisotropy appear to approach the bulk value as the film thickness increases, while the uniaxial anisotropy changes sign from negative to positive.

IV. DISCUSSION

We will first illustrate how the continuous directional change of the net anisotropy axes, which we observed *in situ* for epitaxial Fe/GaAs films, arises from a combination of a uniaxial IPMA and the cubic anisotropy. We then address the thickness dependence of the anisotropies and the magnetization as revealed by BLS measurements and finally discuss possible origins of the uniaxial IPMA which is unexpected for symmetry reasons.

In order to understand the evolution of the IPMA with increasing Fe film thickness, we consider the total magnetic anisotropy energy density for a film of cubic symmetry which is given for the case without an external field up to fourth order by

$$F_{\text{anisotropy}}^{(\text{cubic})} = K_1(\alpha_1^2\alpha_2^2 + \alpha_2^2\alpha_3^2 + \alpha_3^2\alpha_1^2) + K_{u\perp}^{\text{eff}}(t)\sin^2\theta,$$

$$(1)$$

where K_1 denotes the cubic magnetocrystalline bulk anisotropy which according to the Néel approach[2] has no thickness dependence, $K_{u\perp}^{\text{eff}}(t)$ is the thickness dependent uniaxial perpendicular anisotropy which contains contributions from the volume, magnetocrystalline, and magnetoelastic terms as well as the demagnetizing energy which dominates for the films considered here.[25] The α_1, α_2, and α_3 are the direction cosines for the direction of the magnetization with respect to each cubic axis, where α_1 and α_2 refer to in-plane axes, and α_3 to the out-of-plane axis. The angle θ is the angle between the film normal and the magnetization direction. An earlier study[15] does not suggest the existence of a positive perpendicular anisotropy favoring out-of-plane spin alignment. Even if a small surface anisotropy contribution is present, no canting out-of-plane can occur since its axis coincides with the easy axes of the cubic anisotropy (positive in Fe). Thus the total free energy density is minimized for $\theta = 90°$.

Considering only the IPMA, we set $\theta = 90°$ and obtain from Eq. (1) for the (001) surface of a cubic crystal:

$$F_{\text{IPMA}}^{(001)} = \tfrac{1}{4} K_1 \sin^2(2\varphi) \tag{2}$$

and for the $(\bar{1}10)$ surface:

$$F_{\text{IPMA}}^{(\bar{1}10)} = \tfrac{1}{4} K_1 (\tfrac{3}{4} \sin^2(2\varphi) + \sin^2 \varphi) + K_{u\parallel}(t)\sin^2 \varphi, \tag{3}$$

where the second term, which corresponds to a uniaxial IPMA, has to be added for symmetry reasons.[27] The azimuthal angle φ is measured with respect to the [100] and [001] directions for the (001) and $(\bar{1}10)$ surfaces, respectively.

For (001) oriented magnetic films, Eq. (2) contains only a contribution from the constant cubic bulk anisotropy. This is obviously not sufficient to describe the observed continuous evolution of the IPMA in thin Fe/GaAs(001) films. Hence, a thickness dependent uniaxial IPMA, $K_{u\parallel}(t)$, must be added to Eq. (2), and as indicated by the BLS results in Fig. 2, the cubic anisotropy should also depend on t:

$$F_{\text{IPMA}}^{(001)} = \tfrac{1}{4} K_1(t)\sin^2(2\varphi) + K_{u\parallel}(t)\sin^2(\varphi + 45°). \tag{4}$$

The phase shift of 45° takes into account that the uniaxial anisotropy hard axis is parallel to [110] in the thin film limit. In Fig. 6, $F_{\text{IPMA}}^{(001)}$ is plotted qualitatively as a function of the in-plane angle φ for different ratios of $r = K_{u\parallel}(t)/K_1(t)$ and positive values of $K_1(t)$ and $K_{u\parallel}(t)$. The two energy maxima at 45° and 135°, which correspond to the hard magnetization axes, are inequivalent for nonzero uniaxial IPMA (i.e., $|r| > 0$). The [110] axis is labeled as hard–hard (hard cubic +hard uniaxial) and the [$\bar{1}$10] hard–easy (hard cubic+easy uniaxial).[14] The dots denote the angles of the easy axes which are defined by the energy minima. As long as the uniaxial anisotropy dominates, $|r| > 1$, only one easy axis exists parallel to [$\bar{1}$10] in agreement with the MOKE loops for 16 Å in Fig. 1. Two energy minima are present when $|r| < 1$ and these move toward the $\langle 100 \rangle$ directions as r approaches zero, i.e., when the uniaxial IPMA becomes negligible. This is observed for Fe films thicker than 50 Å (e.g., 73 Å in Fig. 1).

For $(\bar{1}10)$ oriented magnetic films, the cubic anisotropy K_1 appearing in Eq. (3) also has a thickness dependence as indicated by the BLS results in Fig. 5:
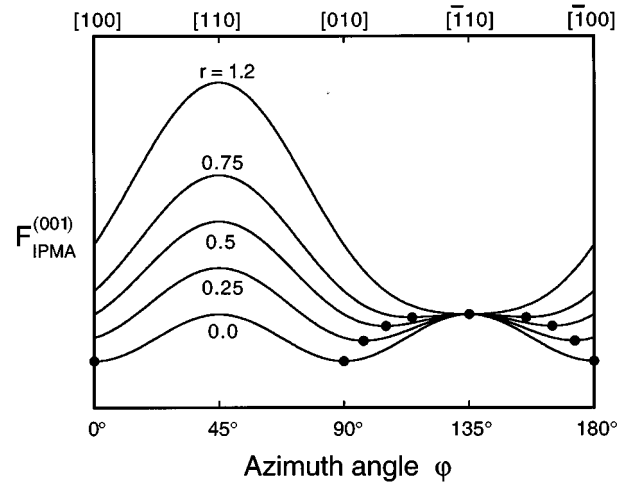

FIG. 6. The in-plane anisotropy energy density according to Eq. (4) at zero field for a (001) oriented magnetic film and different anisotropy ratios $r = K_{u\parallel}/K_1$. The uniaxial hard axis is parallel to [110]. The dots denote the energy minima.

$$F_{\text{IPMA}}^{(\bar{1}10)} = \tfrac{1}{4} K_1(t)(\tfrac{3}{4} \sin^2(2\varphi) + \sin^2 \varphi) + K_{u\parallel}(t)\sin^2 \varphi. \tag{5}$$

In Fig. 7, $F_{\text{IPMA}}^{(\bar{1}10)}$ is plotted qualitatively as function of the in-plane angle φ for different ratios of $r = K_{u\parallel}(t)/K_1(t)$ with $K_1(t) > 0$. Up to the critical anisotropy ratio $r_c = -0.25$ the absolute minimum is at $\varphi = 90°$, which means the easiest axis is parallel to [110] as observed with *in situ* MOKE for thin Fe films (Fig. 3). A second local minimum appears at 0° for $r > -1$ which makes the [001] direction an intermediate axis and gives rise to a kink in the magnetization curve when the external field is reversed (at 66 Å in Fig. 3). For $r = r_c$, the
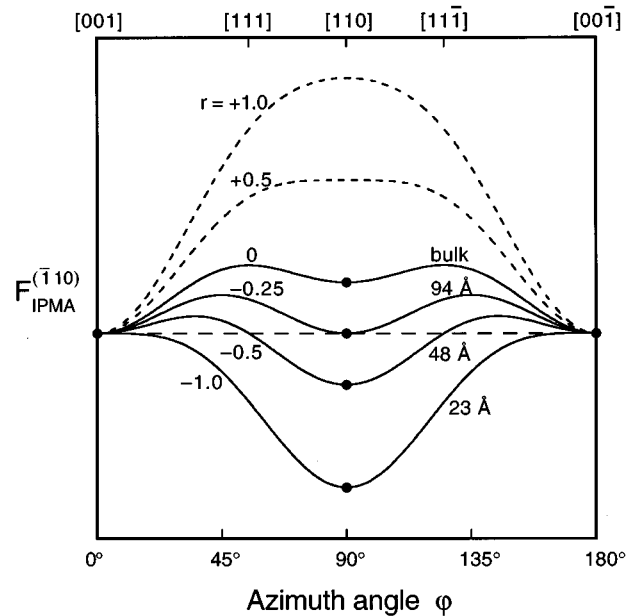

FIG. 7. The in-plane anisotropy energy density at zero field according to Eq. (3) for Fe($\bar{1}10$) films with different anisotropy ratios $r = K_{u\parallel}/K_1$. The solid lines and the thicknesses refer to the case when only a t^{-1} dependent surface anisotropy contributes to $K_{u\parallel}(t)$ and the anisotropy energies are the same as in the case of Fe/W($\bar{1}10$) (Ref. 5). The dots denote the energy minima.

J. Appl. Phys., Vol. 80, No. 1, 1 July 1996

Gester *et al.* 351

energy minima at 0° and 90° have the same value and two equivalent easy axes exist simultaneously (at 118 Å in Fig. 3). For thicker Fe/GaAs($\bar{1}$10) films, the absolute minimum is at $\varphi = 0°$ which means the easiest axis is parallel to [001] as in bulk Fe. The local minimum now at 90° makes the [110] direction an intermediate axis and gives rise to kinks in the MOKE loops (from 145 Å onwards in Fig. 3).

The same switching behavior of the in-plane easy magnetization axis was found in Fe/W($\bar{1}$10) films.[5] The authors used the ansatz for the anisotropy energy density given in Eq. (5) and assumed additionally that the magnetization is homogeneous across the entire film thickness, K_1 is constant and equals the value for bulk Fe ($+4.7 \times 10^5$ erg/cm^3), and $K_{u\parallel}(t)$ arises only from magnetocrystalline interface anisotropy. In this case, $F_{\text{IPMA}}^{(\bar{1}10)}$ depends on the thickness only through the uniaxial IPMA which is given by $K_{u\parallel}(t) = K_{u\parallel}^{(s)} t^{-1}$. Under these assumptions, the strength of the uniaxial IPMA can be easily determined from the critical thickness t_c at which the two equivalent easy axes are observed experimentally. For Fe films on W($\bar{1}$10), t_c was found to be 105 Å and hence $K_{u\parallel}^{(s)} = -0.11$ erg/cm^2.[5] Using this result the anisotropy ratios can be expressed in terms of the Fe film thickness as indicated in Fig. 7. From the series of *in situ* magnetization curves presented in Fig. 3 for an Fe/GaAs($\bar{1}$10) film of 230 Å total thickness we obtain $t_c \approx 120$ Å, while the two easy axes are simultaneously observed at 80 Å for a different film of 100 Å total thickness which was produced in another growth run. The fact that the precise value for the critical thickness depends sensitively on the growth conditions agrees with previously reported results.[11]

However, the assumptions made above for Fe films on W($\bar{1}$10) are not applicable for the Fe/GaAs system. From the BLS results in Fig. 5, it is obvious that neither the magnetization is homogeneous across the entire film thickness nor is the cubic anisotropy constant as in bulk Fe. In addition, if the uniaxial IPMA contains only the Néel type interface anisotropy, the energy maximum in Fig. 7 moves with increasing film thickness from $\varphi = 0°$ toward 55° which corresponds to a shift of the hard anisotropy axis from [001] toward [111], the direction in bulk Fe. However, using *ex situ* MOKE, we established (Fig. 4) that in thick Fe/GaAs($\bar{1}$10) films the hard axis is close to or aligned with the [110] direction in agreement with previous observations.[28] Only if we allow $K_{u\parallel}(t)$ to become increasingly positive, the corresponding maximum of $F_{\text{IPMA}}^{(\bar{1}10)}$ shifts toward 90° and hence the hard magnetization axis is finally parallel to the [110] direction when $K_{u\parallel}(t) \geqslant 0.5 K_1$ (the dashed lines in Fig. 7). The change of sign from negative to positive for $K_{u\parallel}(t)$ is experimentally confirmed by BLS (Fig. 5). For the 230-Å-thick Fe film, the BLS measurements yield $K_{u\parallel}(t) = 0.61 K_1$.[25] Therefore, we can conclude that at least one additional uniaxial IPMA contribution must be present which makes the [110] direction a hard magnetization axis in the thick film limit.

This assumption is further confirmed by magnetization curves calculated using the coherent rotation model.[29] They are shown in Fig. 8 for constant cubic anisotropy K_1 and three different values of the uniaxial IPMA $K_{u\parallel}(t)$ which were derived from the BLS results for the 230-Å-thick Fe
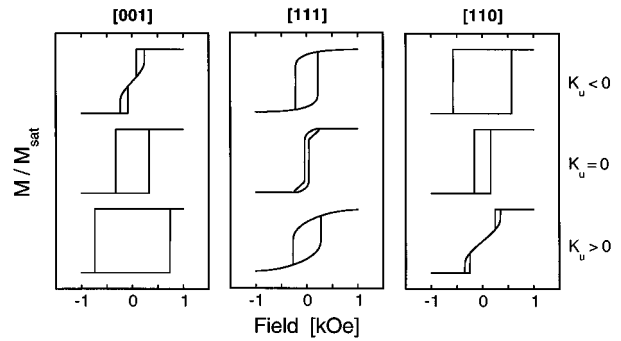

FIG. 8. Calculated magnetization curves for Fe($\bar{1}$10) films with positive cubic anisotropy K_1 and different values of the in-plane uniaxial anisotropy $K_{u\parallel}$.

sample and bulk saturation magnetization. The three sets of loops for different values of $K_{u\parallel}(t)$ reproduce well the shape of the MOKE loops for 66, 118, and 230 Å in Fig. 3, respectively. Also the observed decrease in the coercive field of the square loops along the [110] direction with increasing thickness agrees well with the calculation.

The above considerations of the balance between uniaxial IPMA and cubic anisotropy provide a qualitative explanation for the switching of the anisotropy axes directions as observed *in situ* in Fe films deposited onto GaAs(001) and GaAs($\bar{1}$10) substrates. In both cases, we find a uniaxial IPMA contribution which is not expected from symmetry considerations and of the same order of magnitude as the cubic anisotropy K_1. The quantitative BLS measurements confirm that $K_{u\parallel}(t)$ continues to increase beyond 200 Å in ($\bar{1}$10) oriented Fe films while it drops to zero only at thicknesses over 500 Å in (001) oriented films. The thickness dependence of both the magnetization and the cubic anisotropy is similar for Fe films deposited onto either (001) or ($\bar{1}$10) GaAs substrates. $2K_1/M$ and $(4\pi M)_{\text{eff}}$ are reduced up to about 200 Å and approach the bulk values for large thicknesses.

As mentioned in Sec. I, there are different mechanisms which can give rise to thickness dependent magnetic properties in thin films: (i) reduced symmetry at the surface or the edges of atomic steps, (ii) intermixing of atoms at the interface, and (iii) strain. In the following, we will first introduce these three mechanisms with respect to the Fe–GaAs system and consider their contribution to the observed thickness dependence of the magnetization and the cubic anisotropy.

(i) Besides the surface anisotropy introduced earlier in this section, atomic steps at the surface of a magnetic film give rise to a step anisotropy which is proportional to $\rho_{\text{st}}(t) t^{-1}$. The step density $\rho_{\text{st}}(t)$ is constant for steps at the film–substrate interface, however, at the free surface, $\rho_{\text{st}}(t)$ can change during film growth and depend on the total film thickness. We observed with LEED (Sec. II) that the step density increases during growth in the case of Fe/GaAs(001) and decreases in the case of Fe/GaAs($\bar{1}$10), but the thickness dependence of $2K_1/M$ and $(4\pi M)_{\text{eff}}$ is similar in both cases (Figs. 2 and 5). Therefore, the steps at the surface of the Fe/GaAs films are unlikely to account for the thickness dependence of the magnetization or the cubic anisotropy.

Gester *et al.*

(ii) The presence of As atoms in the Fe matrix was clearly revealed by photoelectron spectroscopy for Fe films deposited onto both GaAs(001)[30,31] and GaAs($\bar{1}$10) substrates.[32] Segregation of As was observed at the surface of about 100-Å-thick Fe films using Auger electron spectroscopy.[20] As pointed out previously,[20] the phase diagram for the Fe–As binary system shows that Fe_2As and As-doped α-Fe will be the dominant phases for low As concentrations. This is believed to account for the observed variation of the magnetization with thickness since any kind of Fe–As compound will modify the electronic structure of the Fe atoms and reduce its magnetic moment. Since the anisotropy energy in bulk Fe scales with the magnetization (the tenth power in the case of the fourth-order cubic bulk anisotropy),[33] K_1 is expected to have a thickness dependence over the same length scale as that of the magnetization in agreement with our BLS results (Figs. 2 and 5).

(iii) Strain in epitaxial films gives rise to magnetoelastic anisotropy which falls as t^{-1} if it is relaxed via dislocations.[34] For symmetry reasons, homogeneous lateral strain in cubic films contributes to the in-plane anisotropy only for ($\bar{1}$10) and not for (001) oriented films. Nevertheless, thickness dependent cubic in-plane anisotropy was previously observed and attributed to strain in systems such as Fe/Ag(001)[35] and Co/Cu(001).[36] Pseudomorphic Fe films on GaAs are compressed due to a lattice mismatch of 1.36%. The analysis of the separation of RHEED streaks for Fe films deposited onto GaAs($\bar{1}$10) suggests that strain is relaxed after 200 Å via dislocations[24] which are on the same length scale as the observed variation of the magnetization and cubic anisotropy. In Fe/GaAs films additional strain can be induced by the As atoms which are found to occupy face centered sites in the bcc Fe lattice.[31] Thus the presence of As in the Fe film can affect the thickness dependence of the magnetic properties not only through chemical but also magnetoelastic interaction.[20]

The unexpected uniaxial IPMA in Fe/GaAs(001) films can be attributed to the structure of the GaAs substrate surface. Removing the surface oxide by ion bombardment followed by annealing retains a Ga terminated GaAs(001) surface. The dangling bonds of the Ga atoms are directed parallel to the [110] direction and break the cubic symmetry at the surface. Pairing of these bonds leads to reconstructions[37] which we clearly identified with LEED.[18] STM images show that the reconstructed Ga-rich (001) surface consists of rows of missing Ga dimers parallel to the [110] direction leading to the formation of trenches 8 Å wide and 2 Å deep.[38] Hence, the undersurface of the Fe film will contain atomic steps with edges parallel to the [110] direction which give rise to a uniaxial IPMA proportional to the inverse film thickness. Our BLS results for $K_{u\parallel}(t)$ (the circles in Fig. 2) follow approximately a t^{-1} dependence as indicated by the dotted line. The fact that the scatter of the data points is greater for the uniaxial anisotropy field than for $2K_1/M$ and $(4\pi M)_{eff}$ underlines the strong influence of the substrate surface on the uniaxial IPMA.

Our assumption of a substrate induced uniaxial IPMA is further supported by the results obtained for Fe films grown on other substrates with a fourfold surface symmetry such as
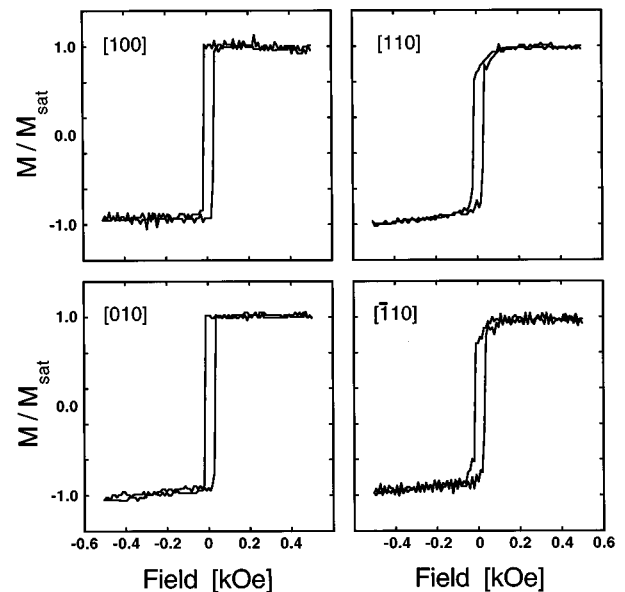

FIG. 9. *In situ* MOKE loops for 12 Å Fe on a Ag(001) buffer layer.

Ag(001). The *in situ* $M-H$ curves in Fig. 9 for a 12-Å-thick Fe film deposited onto an Ag(001) buffer grown on GaAs(001) exhibit fourfold symmetry with the easy axes parallel to the $\langle 100 \rangle$ directions as in bulk Fe. This is clearly different when compared with the MOKE loops for the 16-Å-thick Fe film on GaAs(001) in Fig. 1. Uniaxial IPMA was also not found in thin Fe films on W(001)[39] or MgO(001).[40]

While the sample normal was always parallel to the Fe beam, we found that the uniaxial hard axis is parallel to the [110] direction in all Fe films deposited onto GaAs(001) regardless of the azimuthal orientation during growth. Thus, the possible effect of the geometrical arrangement during growth can be clearly ruled out as the origin of the uniaxial IPMA. The same orientation of the uniaxial hard axis with respect to the step edges was observed in Fe films deposited onto stepped W(001) substrates.[39]

We also investigated the structure of the Fe vacuum interface which was not accessible in previous studies of the Fe/GaAs system but which could also influence the anisotropy behavior. For (001) oriented Fe films, our LEED images clearly reveal the presence of surface steps with edges predominantly parallel to all four $\langle 110 \rangle$ directions.[18] However, we do not believe that the resulting magnetic step anisotropy contributes to the uniaxial IPMA for two reasons: First, the diffraction pattern showed cubic symmetry for all thicknesses with no detectable difference of the spot broadening in either the [110] or [$\bar{1}$10] direction. Second, the LEED spot profiles indicate that the surface roughness and hence the step density increases as the Fe deposition continues which confirms previous observations.[20] We found that the number of steps at the Fe–vacuum interface increases in such a way that the ratio of the roughness amplitude to the total film thickness remains constant.[18] Hence, the step density $\rho_{st}(t)$ is proportional to t and the resulting step anisotropy becomes independent of the film thickness in contrast to our BLS results for $K_{u\parallel}(t)$ (Fig. 2).

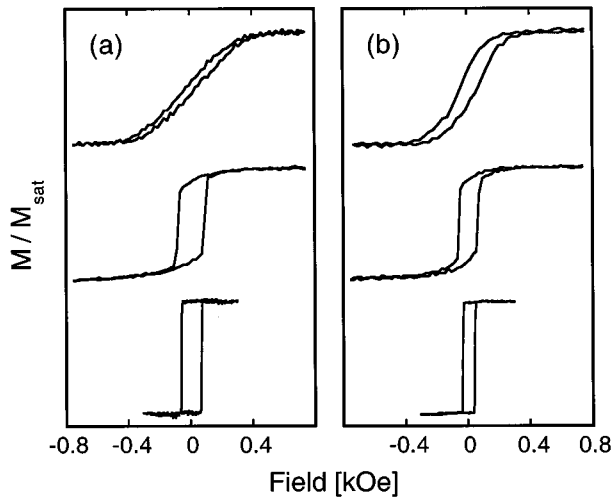As mentioned in Sec. II, we also investigated the influ-

FIG. 10. *In situ* MOKE loops for 17 Å Fe deposited onto (a) a sputter-annealed GaAs(001) substrate and (b) a heated-only substrate.

ence of the substrate preparation method on the properties of the Fe film. In a particular experiment, we mounted a single piece of GaAs(001) onto our sample holder with a mask over one-half. The uncovered half was ion bombarded and the mask removed afterwards. The substrate was then annealed and Fe evaporated onto the whole surface area allowing a direct comparison between films on sputter-annealed and heated-only GaAs without any uncertainties due to slight differences of the substrate material or the annealing temperature. A 17-Å-thick Fe film grown on the sputter-annealed half of the GaAs(001) substrate showed a clear LEED pattern while no diffraction spots were visible for the same Fe film deposited onto the heated-only half. The $M-H$ curves obtained *in situ* for two such Fe films are shown in Fig. 10. In contrast to the film structure, the magnetic properties are very similar. Only the coercivities for the easy $[\bar{1}10]$ and intermediate $[010]$ axis are slightly larger for the Fe film on the ion bombarded and subsequently annealed substrate, indicating that the structural quality of the film is slightly better on this substrate in agreement with the LEED results. The kind of substrate used also does not affect qualitatively the evolution of the anisotropy but the thickness range varies in which the transition from the uniaxial to the cubic dominated anisotropy state occurs.

In view of these results, we conclude for the annealed-only films that crystallographically ordered areas exist on the surface which extend over a length scale too small to be detected with LEED. This implies that the structural length scale responsible for the magnetic anisotropies is extremely small (approximately 25 Å) and explains the sensitivity of the magnetic properties to minute differences in the growth process. This is reflected by the scattering of the data in Figs. 2 and 5, where each point represents a different sample.

The case of Fe films deposited onto GaAs($\bar{1}10$) is more complex because at least two uniaxial IPMA contributions are present as we have shown earlier in this section. Assuming that one contribution is given by the Néel type surface anisotropy, we can write:

$$K_{u\parallel}(t) = \frac{K_{u\parallel}^{(s)}}{t} + K_{u\parallel}^{(2)}(t), \qquad (6)$$

where $K_{u\parallel}^{(S)} < 0$, so that the $[110]$ direction is an easy magnetization axis at small thicknesses. In order to account for the change of sign of $K_{u\parallel}(t)$, $K_{u\parallel}^{(2)}$ must be positive and decrease less rapidly with thickness than t^{-1}.

This requirement rules out the possibility that atomic steps at either Fe interface are the source of the second uniaxial anisotropy contribution $K_{u\parallel}^{(2)}$. Anisotropy arising from steps at the Fe–substrate interface would always be proportional to t^{-1} regardless of the detailed structure at the undersurface. For the free surface of ($\bar{1}10$) oriented Fe films, our RHEED results indicate that the step density $\rho_{st}(t)$ decreases with increasing film thickness and hence a possible uniaxial IPMA would fall more rapidly with thickness than t^{-1}.

Lateral strain in the Fe film due to the lattice mismatch at the interface also cannot account for $K_{u\parallel}^{(2)}$ because it would favor alignment of the magnetization parallel to $[110]$ like $K_{u\parallel}^{(S)}$.[12] Thus the available structural information is not sufficient to explain the continuous shift of the hard axis from the $[111]$ direction toward the $[110]$ in Fe/GaAs($\bar{1}10$) films which we observed with *in situ* MOKE and BLS. However, as we have seen in the case of Fe/GaAs(001) films, the magnetic properties depend on structural features which extend only over few atoms which cannot be observed with LEED. It is also possible that the parametrization in Eq. (6) is not sufficient.

V. SUMMARY

We show in this article that the magnetic properties of epitaxial Fe single films on GaAs(001) and ($\bar{1}10$) substrates vary continuously with increasing film thickness using the magneto-optic Kerr effect during film deposition. The in-plane anisotropy fields are quantitatively measured for a selection of Cr coated Fe films using BLS. In Fe films of both orientations, we find a uniaxial IPMA contribution which is unexpected for symmetry reasons. In the case of Fe/GaAs(001) films, we identify steps at the GaAs–Fe interface due to the substrate surface structure as the source of the uniaxial IPMA. From our LEED study, we conclude that steps at the top surface of the (001) oriented Fe films are not responsible for the uniaxial IPMA. Homogeneous lateral strain or steps at the interfaces cannot account for the uniaxial anisotropy behavior which we observed in Fe/GaAs($\bar{1}10$) films. Finally, the comparison of magnetic properties in Fe films deposited onto GaAs with different degrees of crystalline order at the substrate surfaces allows us to conclude that the magnetic anisotropies in thin films are determined by atomic scale order.

ACKNOWLEDGMENTS

[1] *Ultrathin Magnetic Structures*, edited by B. Heinrich and J. A. C. Bland (Springer, Berlin, 1994), Vol. I, Chap. 2.

[2] M. L. Néel, J. Phys. Rad. **15**, 225 (1954).

[3] C. Chappert and P. Bruno, J. Appl. Phys. **64**, 5736 (1988).

[4] P. Bruno, J. Appl. Phys. **64**, 3153 (1988).

[5] U. Gradmann, J. Korecki, and G. Waller, Appl. Phys. A **39**, 101 (1986).

[6] B. Hillebrands and J. R. Dutcher, Phys. Rev. B **47**, 6126 (1993).

[7] M. Albrecht, T. Furubayashi, M. Przybylski, J. Korecki, and U. Gradmann, J. Magn. Magn. Mater. **113**, 207 (1992).

[8] J. Faßbender, C. Mathieu, B. Hillebrands, G. Güntherodt, R. Jungblut, and M. T. Johnson, J. Magn. Magn. Mater. **148**, 156 (1995).

[9] B. Hillebrands, J. Faßbender, R. Jungblut, G. Güntherodt, D. J. Roberts, and G. A. Gehring, Phys. Rev. B **53**, 10548 (1996).

[10] G. A. Prinz, Science **250**, 1092 (1990).

[11] G. A. Prinz, G. T. Rado, and J. J. Krebs, J. Appl. Phys. **53**, 2087 (1982).

[12] J. J. Krebs, F. J. Rachford, P. Lubitz, and G. A. Prinz, J. Appl. Phys. **53**, 8085 (1982).

[13] J. M. Florczak and E. D. Dahlberg, Phys. Rev. B **44**, 9338 (1991).

[14] C. Daboo, R. J. Hicken, E. Gu, M. Gester, S. J. Gray, D. E. P. Eley, E. Ahmed, J. A. C. Bland, R. Ploessl, and J. N. Chapman, Phys. Rev. B **51**, 15964 (1995).

[15] K. T. Riggs, E. D. Dahlberg, and G. A. Prinz, J. Magn. Magn. Mater. **73**, 46 (1988).

[16] J. G. Gay and R. Richter, Phys. Rev. Lett. **56**, 2728 (1986).

[17] M. Stampanoni, A. Vaterlaus, M. Aeschlimann, and F. Meier, Phys. Rev. Lett. **59**, 2483 (1987).

[18] M. Gester, S. J. Gray, C. Daboo, E. Gu, and J. A. C. Bland (unpublished).

[19] E. Gu, J. A. C. Bland, C. Daboo, M. Gester, L. M. Brown, R. Ploessl, and J. N. Chapman, Phys. Rev. B **51**, 3596 (1995).

[20] J. J. Krebs, B. T. Jonker, and G. A. Prinz, J. Appl. Phys. **61**, 2596 (1987).

[21] P. Drahten, W. Ranke, and K. Jacobi, Surf. Sci. **77**, L162 (1978).

[22] O. Durand, J. R. Childress, P. Galtier, R. Bisaro, and A. Schuhl, J. Magn. Magn. Mater. **145**, 111 (1995).

[23] P. Etienne, S. Lequien, F. Nguyen-Van-Dau, R. Cabanel, G. Creuzet, A. Friederich, J. Massies, A. Fert, A. Barthélémy, and F. Petroff, J. Appl. Phys. **67**, 5400 (1990).

[24] G. A. Prinz and J. J. Krebs, Appl. Phys. Lett. **39**, 397 (1981).

[25] R. J. Hicken, D. E. P. Eley, M. Gester, S. J. Gray, C. Daboo, A. J. R. Ives, and J. A. C. Bland, J. Magn. Magn. Mater. **145**, 278 (1995).

[26] J. M. Florczak and E. D. Dahlberg, J. Appl. Phys. **67**, 7520 (1990).

[27] G. T. Rado and L. Zhang, Phys. Rev. B **33**, 5080 (1986).

[28] K. T. Riggs, E. D. Dahlberg, and G. A. Prinz, Phys. Rev. B **41**, 7088 (1990).

[29] B. Dieny, J. P. Gavigan, and J. P. Rebouillat, J. Phys.: Condens. Matter **2**, 159 (1990).

[30] J. R. Waldrop and R. W. Grant, Appl. Phys. Lett. **34**, 630 (1979).

[31] S. A. Chambers, F. Xu, H. W. Chen, I. M. Vitomirov, S. B. Anderson, and J. H. Weaver, Phys. Rev. B **34**, 6605 (1986).

[32] M. W. Ruckman, J. J. Joyce, and J. H. Weaver, Phys. Rev. B **33**, 7029 (1986).

[33] I. S. Jacobs and C. P. Bean, in *Magnetism*, edited by G. T. Rado and H. Suhl (Academic, New York, 1967).

[34] P. Bruno and J. Renard, Appl. Phys. A **49**, 499 (1989).

[35] B. Heinrich, Z. Celinski, J. F. Cochran, A. S. Arrott, and K. Myrtle, J. Appl. Phys. **70**, 5769 (1991).

[36] M. Kowalewski, C. M. Schneider, and B. Heinrich, Phys. Rev. B **47**, 8748 (1993).

[37] D. K. Biegelsen, R. D. Bringans, J. E. Northrup, and L. Swartz, Phys. Rev. B **41**, 5701 (1990).

[38] Q. K. Xue, T. Hashizume, J. M. Zhou, T. Sakata, T. Ohno, and T. Sakurai, Phys. Rev. Lett. **74**, 3177 (1995).

[39] J. Chen and J. L. Erskine, Phys. Rev. Lett. **68**, 1212 (1992).

[40] O. Kohmoto and C.A. Alexander Jr., Jpn. J. Appl. Phys. **31**, 2101 (1992).

J. Appl. Phys., Vol. 80, No. 1, 1 July 1996

Gester *et al.* 355